

DOA TRACKING VIA SIGNAL-SUBSPACE PROJECTOR UPDATE

Jie Zhuang^{1,2}, Tianhan Tan¹, Daolin Chen¹, and Jiancheng Kang¹

¹School of Information and Communication Engineering,
University of Electronic Science and Technology of China (UESTC), Chengdu, China

²Precision Measurement Radar System Technology Key Laboratory of Sichuan Province, Chengdu, China

ABSTRACT

We develop a novel direction-of-arrival (DOA) tracking method in which we directly operate the signal-subspace projector instead of tracking the subspace eigenbasis. In each time frame, we employ a multidimensional subspace fitting approach to track the signal-subspace projector and the DOA measurements can be obtained as a byproduct. Then these measurements are fed into a Kalman filter to produce the refined DOA estimations. Numerical results demonstrate the superior performance of the proposed tracking method relative to the PAST-based methods.

Index Terms— Direction-of-arrival (DOA) tracking, multidimensional subspace fitting, subspace projector, projection approximation subspace tracking algorithm (PAST).

1. INTRODUCTION

Consider an array of N sensors tracking M narrowband sources. The $N \times 1$ signal vector received at the time instant t can be expressed as

$$\mathbf{z}(t) = \mathbf{A}(t)\mathbf{m}(t) + \mathbf{n}(t) \quad (1)$$

where $\mathbf{m}(t)$ collects the M complex narrowband signal envelopes and $\mathbf{n}(t)$ represents the additive white Gaussian noise with covariance $\sigma_n^2 \mathbf{I}$ (σ_n^2 is the noise power). The notation \mathbf{I} denotes an identity matrix. The matrix $\mathbf{A}(t)$ consists of the steering vectors of the M sources, i.e., $\mathbf{A}(t) = [\mathbf{a}(\theta_1(t)), \dots, \mathbf{a}(\theta_M(t))]$ where $\mathbf{a}(\theta(t))$ represents the steering vector associated with the azimuth angle $\theta(t) \in [0, 2\pi)$. Here we assume that the azimuth angles $\{\theta_m(t)\}_{m=1}^M$ are time-varying but remain approximately constant over each time frame so that $\theta_m(t) \approx \theta_m(k)$ for $t \in [kT, (k+1)T)$ where $k = 1, 2, \dots, K$. During each time interval T , N_s snapshots are collected. The direction-of-arrival (DOA) tracking problem which we will deal with in this paper can now be briefly stated as follows: during each time frame use the N_s snapshots to estimate the DOAs $\{\theta_m(k)\}_{m=1}^M$ while preserving the association between the

previous DOAs $\{\theta_m(k-1)\}_{m=1}^M$ and the current DOAs $\{\theta_m(k)\}_{m=1}^M$.

In time-variant scenarios, the conventional subspace-based DOA finding methods (e.g., the well-known MUSIC and ESPRIT algorithms) are impracticable since the computationally expensive eigendecomposition has to be conducted over and over again to obtain the time-variant subspace [1, 2]. In order to reduce the computational complexity, subspace tracking is a natural solution. For instance, the projection approximation subspace tracking (PAST) algorithm [3] attempts to find the subspace eigenbasis by minimizing the following optimization problem

$$J(\mathbf{W}) = E \{ \|\mathbf{z} - \mathbf{W}\mathbf{W}^H \mathbf{z}\|^2 \} \quad (2)$$

where $E\{\cdot\}$ denotes expectation and $\mathbf{W} \in \mathcal{C}^{N \times M}$ is a full-rank matrix to be found. When each new snapshot arrives, the matrix \mathbf{W} can be updated by the gradient method. Once the N_s snapshots are used, the noise-subspace projector associated with the k -th time frame can be computed by $\mathbf{\Pi}_n(k) = \mathbf{I} - \mathbf{W}(k)\mathbf{W}^H(k)$. Subsequently, the following one-dimensional cost function is considered to estimate the DOAs [4]:

$$f(\theta) = \mathbf{a}^H(\theta)\mathbf{\Pi}_n(k)\mathbf{a}(\theta). \quad (3)$$

Provided the predicted DOA $\hat{\theta}_m(k/k-1)$ as an initial value, we can use the Newton-type method to solve (3), which produces the measurement for the current time frame as follows:

$$\tilde{\theta}_m(k) = \hat{\theta}_m(k/k-1) - \frac{\text{Re} \{ \mathbf{d}^H(\theta)\mathbf{\Pi}_n(k)\mathbf{a}(\theta) \}}{\mathbf{d}^H(\theta)\mathbf{\Pi}_n(k)\mathbf{d}(\theta)} \Big|_{\theta=\hat{\theta}_m(k/k-1)} \quad (4)$$

where $\text{Re}\{\cdot\}$ denotes the real part of the argument between braces, and $\mathbf{d}(\theta) = \frac{\partial \mathbf{a}(\theta)}{\partial \theta}$. Then the above measured DOAs are refined by a Kalman filter or Luenberger observer to yield the final estimates. The similar methods are also employed in [5, 6, 7, 8, 9].

In this work, we propose a novel DOA tracking method, which differs from the aforementioned methods in that: 1) we directly track the signal-subspace projector instead of its eigenbasis, 2) the DOA estimation is incorporated into the signal-subspace projector updating whereas two stages

This work was supported by National Natural Science Foundation of China (NSFC) under Grant 61571090.

(eigenbasis tracking and DOA measurement finding in (4)) are needed for the PAST-based methods. Since the essence of our proposed method is based on multidimensional subspace fitting, our method can achieve better estimation performance than the one-dimensional methods.

2. PROPOSED DOA TRACKING METHOD

2.1. Tracking using the signal-subspace projector

It is found in [3] that the optimal solution of (2) is not uniquely determined when we minimize $J(\mathbf{W})$. However, the outer product $\mathbf{W}\mathbf{W}^H$ is unique and it equals the signal-subspace projection matrix. Motivated by this observation, we can obtain the following multidimensional subspace fitting problem by replacing $\mathbf{W}\mathbf{W}^H$ with the signal-subspace projector $\mathbf{\Pi}_s$ [10]

$$\begin{aligned} J(\mathbf{\Pi}_s) &= E \{ \|\mathbf{z} - \mathbf{\Pi}_s \mathbf{z}\|^2 \} \\ &= \text{Tr} \{ \mathbf{R}_x - \mathbf{\Pi}_s \mathbf{R}_x - \mathbf{\Pi}_s^H \mathbf{R}_x + \mathbf{\Pi}_s^H \mathbf{\Pi}_s \mathbf{R}_x \} \end{aligned} \quad (5)$$

where $\text{Tr}\{\cdot\}$ denotes the trace of the matrix argument, the covariance matrix \mathbf{R}_x can be estimated by

$$\hat{\mathbf{R}}_x = \frac{1}{N_s} \sum_{n=1}^{N_s} \mathbf{z}(n) \mathbf{z}^H(n) \quad (6)$$

and the projector $\mathbf{\Pi}_s$ of the k -th time frame can be computed by

$$\mathbf{\Pi}_s(k) = \mathbf{A}(k) \mathbf{A}^\dagger(k) \quad (7)$$

with $\mathbf{A}^\dagger(k) = (\mathbf{A}^H(k) \mathbf{A}(k))^{-1} \mathbf{A}^H(k)$ denoting the Moore-Penrose pseudo-inverse. Using the property $\mathbf{\Pi}_s^H = \mathbf{\Pi}_s$ and the fact $\text{Tr}\{\mathbf{\Pi}_s \mathbf{R}_x\} = \text{Tr}\{\mathbf{R}_x \mathbf{\Pi}_s\}$, (5) can be rewritten as

$$J(\mathbf{\Pi}_s) = \text{Tr} \{ \mathbf{R}_x \mathbf{\Pi}_s^2 - 2 \mathbf{R}_x \mathbf{\Pi}_s + \mathbf{R}_x \}. \quad (8)$$

Differentiating (8) with respect to the m -th ($m = 1, 2, \dots, M$) DOA, we can find the m -th element of the gradient vector as

$$[\nabla J(\mathbf{\Pi}_s)]_m = \text{Tr} \left\{ (\mathbf{\Pi}_s \mathbf{R}_x + \mathbf{R}_x \mathbf{\Pi}_s - 2 \mathbf{R}_x) \frac{\partial \mathbf{\Pi}_s}{\partial \theta_m} \bigg|_{\Theta_0} \right\} \quad (9)$$

where $\Theta_0 = [\theta_{1,0}, \theta_{2,0}, \dots, \theta_{M,0}]^T$ stands for the starting point. The first derivative of the projector with respect to the azimuth angle θ_m is given by [11, 12]

$$\begin{aligned} \frac{\partial \mathbf{\Pi}_s}{\partial \theta_m} &= (\mathbf{I} - \mathbf{\Pi}_s) \frac{\partial \mathbf{A}(k)}{\partial \theta_m} \mathbf{A}^\dagger(k) + (\dots)^H \\ &= (\mathbf{I} - \mathbf{\Pi}_s) \frac{\partial \mathbf{a}(\theta)}{\partial \theta_m} [\mathbf{A}^\dagger(k)]_{m,:} + (\dots)^H \end{aligned} \quad (10)$$

where the notation $(\dots)^H$ means that the same expression appears again with conjugate transpose, and $[\mathbf{A}^\dagger(k)]_{m,:}$ denotes the m -th row of $\mathbf{A}^\dagger(k)$. Furthermore, the (m, q) -th element

of the Hessian matrix is given by (11), shown at the top of the next page, with $m, q = 1, 2, \dots, M$.

By the Gauss-Newton principle [13, 14, 15], we can drop the second derivative terms in (11) to obtain

$$\begin{aligned} &[\nabla^2 J(\mathbf{\Pi}_s)]_{m,q} \\ &\approx \text{Tr} \left\{ \left(\frac{\partial \mathbf{\Pi}_s}{\partial \theta_q} \bigg|_{\Theta_0} \mathbf{R}_x + \mathbf{R}_x \frac{\partial \mathbf{\Pi}_s}{\partial \theta_q} \bigg|_{\Theta_0} \right) \frac{\partial \mathbf{\Pi}_s}{\partial \theta_m} \bigg|_{\Theta_0} \right\}. \end{aligned} \quad (12)$$

and consequently the residual vector $\Delta \Theta = [\Delta \theta_1, \Delta \theta_2, \dots, \Delta \theta_M]^T$ can be computed by

$$\Delta \Theta = -[\nabla^2 J(\mathbf{\Pi}_s)]^{-1} \nabla J(\mathbf{\Pi}_s). \quad (13)$$

2.2. Kalman Filter

Now we can obtain the DOA measurements by (13) if we take the predicted DOAs as the starting point. Then we can apply a Kalman filter to smooth the DOAs. Following the work of [16], we define the state vector of the m -th source at the k -th time frame as $\mathbf{x}_m(k) \triangleq [\theta_m(k) \ \dot{\theta}_m(k) \ \ddot{\theta}_m(k)]^T$ where $\dot{\theta}_m(k)$ and $\ddot{\theta}_m(k)$ are, respectively, the velocity and acceleration of $\theta_m(k)$. In addition, the dynamics and the measurement equations of the m -th target can be modeled as

$$\begin{aligned} \mathbf{x}_m(k) &= \mathbf{F} \mathbf{x}_m(k-1) + \mathbf{w}_m(k) \\ y_m(k) &= \mathbf{h}^T \mathbf{x}_m(k) + v_m(k) \end{aligned} \quad (14)$$

where

$$\mathbf{F} = \begin{bmatrix} 1 & T & \frac{T^2}{2} \\ 0 & 1 & T \\ 0 & 0 & 1 \end{bmatrix} \quad (15)$$

is the state transition matrix and $\mathbf{h} = [1 \ 0 \ 0]^T$. We assume that the noise process $\mathbf{w}_m(k)$ and the measurement noise $v_m(k)$ are both normally distributed with zero mean. The covariance matrix of $\mathbf{w}_m(k)$ is represented by $\mathbf{Q}_m(k)$ (i.e., $\mathbf{Q}_m(k) = E\{\mathbf{w}_m(k) \mathbf{w}_m^H(k)\}$) and the variance of $v_m(k)$ by $\sigma_{y_m}^2(k)$.

Assuming that we have already obtained the state vector $\hat{\mathbf{x}}_m(k-1/k-1)$ and its covariance matrix $\hat{\mathbf{P}}_m(k-1/k-1)$ of the $(k-1)$ -th time frame, the proposed algorithm can be presented as a series of steps as follows:

1. Collect the snapshots to estimate the covariance matrix $\hat{\mathbf{R}}$ by (6) for the k -th time frame.
2. Obtain the predicted state by $\hat{\mathbf{x}}_m(k/k-1) = \mathbf{F} \hat{\mathbf{x}}_m(k-1/k-1)$ and take the first element of $\hat{\mathbf{x}}_m(k/k-1)$ as the predicted DOA $\hat{\theta}_m(k/k-1)$ where $m = 1, 2, \dots, M$.
3. Compute the DOA measurement vector $\tilde{\Theta}(k) = [\tilde{\theta}_1(k), \tilde{\theta}_2(k), \dots, \tilde{\theta}_M(k)]^T$ by

$$\tilde{\Theta} = \hat{\Theta}(k/k-1) + \Delta \Theta \quad (16)$$

where the m -th element of $\hat{\Theta}(k/k-1)$ is $[\hat{\Theta}(k/k-1)]_m = \hat{\theta}_m(k/k-1)$ and $\Delta \Theta$ is calculated by (13)

$$[\nabla^2 J(\mathbf{\Pi}_s)]_{m,q} = \text{Tr} \left\{ \left(\frac{\partial \mathbf{\Pi}_s}{\partial \theta_q} \Big|_{\Theta_0} \mathbf{R}_x + \mathbf{R}_x \frac{\partial \mathbf{\Pi}_s}{\partial \theta_q} \Big|_{\Theta_0} \right) \frac{\partial \mathbf{\Pi}_s}{\partial \theta_m} \Big|_{\Theta_0} \right\} + \text{Tr} \left\{ (\mathbf{\Pi}_s \mathbf{R}_x + \mathbf{R}_x \mathbf{\Pi}_s - 2\mathbf{R}_x) \frac{\partial^2 \mathbf{\Pi}_s}{\partial \theta_m \partial \theta_q} \Big|_{\Theta_0} \right\} \quad (11)$$

with Θ_0 replacing by $\Theta(k/k-1)$ and $\nabla^2 J(\mathbf{\Pi}_s)$ approximated by (12).

4. If $(\delta_m^2(k)/\beta_m(k)) > \gamma$ where $\delta_m(k) \triangleq \tilde{\theta}_m(k) - \hat{\theta}_m(k/k-1)$ and $\beta_m(k)$ can be approximated by $\beta_m(k-1)$, use $\hat{\theta}_m(k/k-1)$ to replace $\tilde{\theta}_m$. The initial β can be set as one.
5. Calculate the measurement variance by $\hat{\sigma}_{y_m}^2(k) = \frac{1}{L} \sum_{j=k-L+1}^k \delta_m(j) \delta_m^*(j)$ where L is the maximum of available sample number.
6. Compute $\hat{\mathbf{Q}}_m(k-1) = \frac{1}{L} \sum_{j=k-L}^{k-1} \mathbf{e}_m(j) \mathbf{e}_m^H(j)$ where $\mathbf{e}_m(k) = \hat{\mathbf{x}}_m(k/k) - \mathbf{F} \hat{\mathbf{x}}_m(k-1/k-1)$, and use $\hat{\mathbf{Q}}_m(k-1)$ to approximate $\hat{\mathbf{Q}}_m(k)$.
7. Calculate $\hat{\mathbf{P}}_m(k/k-1) = \mathbf{F} \hat{\mathbf{P}}_m(k-1/k-1) \mathbf{F}^H + \hat{\mathbf{Q}}_m(k)$.
8. Obtain the Kalman filter gain $\mathbf{g} = \hat{\mathbf{P}}_m(k/k-1) \mathbf{h} / \beta_m(k)$ where $\beta_m(k) = \mathbf{h}^T \hat{\mathbf{P}}_m(k/k-1) \mathbf{h} + \hat{\sigma}_{y_m}^2(k)$.
9. Update the state and the associated covariance matrix by $\hat{\mathbf{x}}_m(k/k) = \hat{\mathbf{x}}_m(k/k-1) + (\tilde{\theta}_m(k) - \hat{\theta}_m(k/k-1)) \mathbf{g}$ and $\hat{\mathbf{P}}_m(k/k) = \hat{\mathbf{P}}_m(k/k-1) - \mathbf{g} \mathbf{h}^T \hat{\mathbf{P}}_m(k/k-1)$.
10. Output the first element of $\hat{\mathbf{x}}_m(k/k)$ as the refined DOA estimation of the k -th time frame, i.e., $\hat{\theta}_m(k/k)$.

Remark 1: The PAST-based method belongs to the one-dimensional problems since only one optimization variable, θ , is considered in (3). In comparison, all the M azimuth angles are taken into account when we minimize the cost function of (8). If we impose the idempotent condition $\mathbf{\Pi}_s = \mathbf{\Pi}_s^2$ on (8), we have $J(\mathbf{\Pi}_s) = \text{Tr}\{(\mathbf{I} - \mathbf{\Pi}_s) \mathbf{R}_s\}$ which becomes the maximum likelihood estimator. As a result, the proposed multidimensional subspace fitting method is expected to have better estimation performance than the one-dimensional methods. Moreover, we deliberately keep the quadratic form in (8) such that we can use the Gauss-Newton method. In comparison with the Newton-type method, the problems of choosing stepsize and computing the full Hessian matrix are both circumvented in our proposed method.

Remark 2: Due to the small dimension of the Kalman filter (i.e., M), the computation complexities of Step 2 and Step 4-10 are negligible. The major computational demand of the proposed algorithm comes from Step 1 and 3 which require

$O(N_s N^2)$ and $O(MN^3 + M^3)$ complexity multiplications respectively, whereas the major computational complexity of the PAST-based methods is $O(\rho M N N_s)$ for the eigenbasis tracking (where $\rho = 3$ or 4). Due to the fact $M < N < N_s$, the computational cost of the proposed method is higher than that of the PAST-based approaches. However, the computation complexity of our proposed method is moderate since the major computational demand is computing the covariance matrix in Step 1 if $N_s > MN$ (which is satisfied in the simulation scenarios).

Remark 3: When the target locations are mutually close, large estimation errors may appear, which leads to excessive error accumulation and even tracking failure. In order to exclude such adverse estimations, we propose to use a validation gate [17, 18, 19] in Step 4 where the threshold γ is taken from the inverse chi-square distribution with one degree of freedom and at a level of α . The value of α is set as 0.95 in our simulation experiments.

3. SIMULATION RESULTS

Assume that three sources are incident on a uniform linear array with $N = 10$ isotropic sensors and half-wavelength sensor spacing. The three sources have equal powers. The time interval is $T = 0.5$ s. In Fig. 1, the true trajectories are illustrated, where we can see that the three sources are crossing each other. To initialize the Kalman filter, we use the traditional MUSIC algorithm to estimate the DOAs for the first two time frames (which are denoted by $\hat{\theta}_m(1)$ and $\hat{\theta}_m(2)$) and these DOAs are shared by the PAST-based methods [4] and our proposed method. Furthermore, we assume that the initial state vector is $\hat{\mathbf{x}}_m(2/2) = [\hat{\theta}_m(2) \quad \frac{\hat{\theta}_m(2) - \hat{\theta}_m(1)}{T} \quad 0]^T$ and the corresponding covariance matrices are given by

$$\hat{\mathbf{P}}_m(2/2) = \begin{bmatrix} 1 & 1/T & 0 \\ 1/T & 2/T^2 & 0 \\ 0 & 0 & 0 \end{bmatrix} \hat{\sigma}_{y_m}^2(2) \quad (17)$$

and

$$\hat{\mathbf{Q}}_m(2) = \begin{bmatrix} T^4/4 & T^3/2 & T^2/2 \\ T^3/2 & T^2 & T \\ T^2/2 & T & 1 \end{bmatrix} \hat{q}_m^2(2). \quad (18)$$

The initial values of $\hat{\sigma}_{y_m}^2(2)$ and $\hat{q}_m^2(2)$ are not critical and thus we can set any two small positive numbers for them [16] (say 10^{-4}).

In the first example, the input signal-to-noise (SNR) ratio of each source varies from 0dB to 30dB while the snapshot

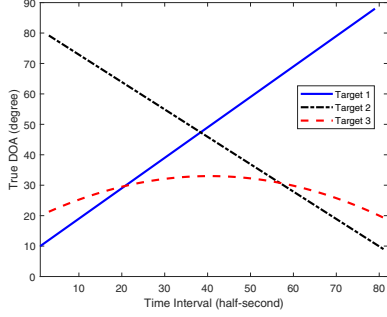


Fig. 1. True trajectories of three targets.

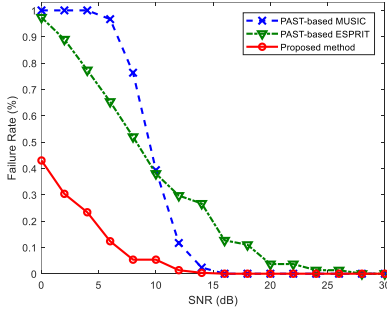


Fig. 2. Failure rate versus SNR; $N_s = 200$.

number (or sample support) during each time frame is fixed at $N_s = 200$. The total number of trials is 300. The methods tested are the proposed method, the PAST-based MUSIC [4] and ESPRIT tracking methods. For the ESPRIT method [20, 21], the DOA measurement for the current time frame corresponds to the eigenvalues of the matrix $(\mathbf{U}_1^H \mathbf{U}_1)^{-1} \mathbf{U}_1^H \mathbf{U}_2$, where \mathbf{U}_1 is obtained by eliminating the last row the signal eigenbasis matrix (which is computed by the PAST algorithm), and \mathbf{U}_2 by eliminating the first row.

We plot the tracking failure rates in Fig. 2 where we can see that in the low-SNR scenarios our proposed method can achieve much lower failure rate than the PAST-based methods. Here the tracking failure rate is defined as the ratio between the failure number and the total trial number. In Fig. 3, we compare the three methods in terms of the DOA estimation root-mean-square errors (RMSEs). For reference, the Cramér-Rao lower bound (CRLB) is also plotted. As illustrated in Fig. 3, the proposed method outperforms the PAST-based methods.

Our second example corresponds to the scenario where the SNR is fixed at 30dB and all other parameters are chosen as in the first example. In such high-SNR situation, the failure rates of tracking tend to zero for all the tracking methods. In Fig. 4, we show the RMSEs at different time frames. Again, we can see that our proposed method works consistently better than the PAST-based methods. It is interesting

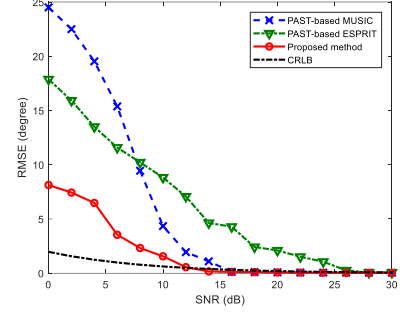


Fig. 3. RMSE versus SNR; $N_s = 200$.

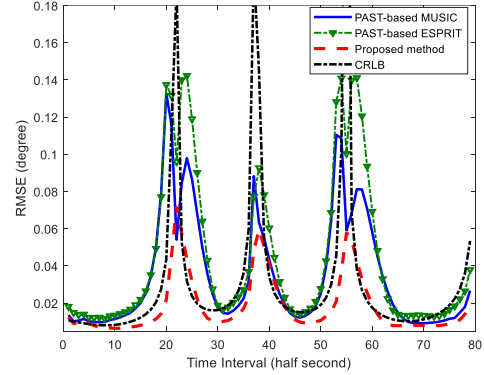


Fig. 4. RMSE versus time interval; $N_s = 200$, SNR=30dB.

to find that the RMSEs of the tested methods are lower than the CRLB at the cross-over time intervals. This can be explained by the fact that the tracking methods have memory, whereas the CRLB is computed without recourse to the previous DOAs. In addition, posterior Cramér-Rao lower bound (PCRLB) [22] may be a better benchmark for this case.

4. CONCLUSIONS

A novel DOA tracking method is proposed in this paper in which we no longer need to track the eigenbasis of the signal subspace. First we form a multidimensional subspace fitting problem which tends to track the subspace projector instead of its eignbasis in each time frame. Then we employ the Gauss-Newton method to solve this optimization problem and the DOA measurements can be obtained as a byproduct. In addition, a Kalman filter with validation gates are proposed to exclude the measurements with large errors when the targets are mutually close. It is worth pointing out that our proposed approach can be readily extended to the situation of two dimensional tracking (i.e., tracking the azimuth and elevation angles simultaneously).

5. REFERENCES

- [1] J. Zhuang, W. Li, and A. Manikas, "An IDFT-based root-MUSIC for arbitrary arrays," *IEEE Int. Conf. Acoustics Speech and Signal Processing (ICASSP)*, pp. 2614–2617, Mar. 2010.
- [2] J. Zhuang, W. Li and A. Manikas, "Fast root-MUSIC for arbitrary arrays," *Electron. Lett.*, vol. 46, no. 2, pp. 174–176, Jan. 2010.
- [3] B. Yang, "Projection approximation subspace tracking," *IEEE Trans. Signal Process.*, vol. 43 no. 1, pp. 95–107, Jan. 1995.
- [4] J. Sanchez-Araujo and S. Marcos, "An efficient PASTd-algorithm implementation for multiple direction of arrival tracking," *IEEE Trans. Signal Process.*, vol. 47 no. 8, pp. 2321–2324, Aug. 1999.
- [5] G. Wang, J. Xin, J. Wang, N. Zheng and A. Sano, "Subspace-based two-dimensional direction estimation and tracking of multiple targets," *IEEE Trans. Aerosp. Electron. Syst.* vol. 51, no. 2, pp. 1386–1402, Apr. 2015.
- [6] J. Xin, N. Zheng and A. Sano, "Subspace-based adaptive method for estimating direction-of-arrival with Luenberger observer," *IEEE Trans. Signal Process.*, vol. 59, no. 1, pp. 145–159, Jan. 2011.
- [7] B. Liao, Z. Zhang and S. Chan, "DOA estimation and tracking of ULAs with mutual coupling," *IEEE Trans. Aerosp. Electron. Syst.*, vol. 48, no. 1, pp. 891–905, Jan. 2012.
- [8] J. Xin and A. Sano, "Efficient subspace-based algorithm for adaptive bearing estimation and tracking," *IEEE Trans. Signal Process.*, vol. 53, no. 12, pp. 4485–4505, Dec. 2005.
- [9] W. Zuo, J. Xin, H. Ohmori, N. Zheng, and A. Sano, "Subspace-based algorithms for localization and tracking of multiple near-field sources," *IEEE J. Sel. Topics Signal Process.*, vol. 13, no. 1, pp. 156–171, Mar. 2019.
- [10] W. Utschick, "Tracking of signal subspace projectors," *IEEE Trans. Signal Process.*, vol. 50, no. 4, pp. 769–778, Apr. 2002.
- [11] M. Viberg and B. Ottersten, "Sensor array processing based on subspace fitting," *IEEE Trans. Signal Process.*, vol. 39, no. 5, pp. 1110–1121, May 1991.
- [12] J. Zhuang, C. Duan, W. Wang and Z. Chen, "Joint estimation of azimuth and elevation via manifold separation for arbitrary array structures," *IEEE Trans. Veh. Technol.*, vol. 67, no. 7, pp. 5585–5596, Jul. 2018.
- [13] S. Boyd and L. Vandenberghe, *Convex optimization*, Cambridge University Press, 2004.
- [14] J. Nocedal and S. J. Wright, *Numerical Optimization*, Second ed., Springer New York, 2006.
- [15] J. Zhuang, H. Xiong, W. Wang and Z. Chen, "Application of manifold separation to parametric localization for incoherently distributed sources," *IEEE Trans. Signal Process.*, vol. 66, no. 11, pp. 2849–2860, Jun., 2018.
- [16] H. Yan and H. H. Fan, "Signal-selective DOA tracking for wideband cyclostationary sources," *IEEE Trans. Signal Process.*, vol. 55, no. 5, pp. 2007–2015, May 2007.
- [17] P. Konstantinova, A. Udvarov and T. Semerdjiev, "A study of a target tracking algorithm using global nearest neighbor approach," *Proceedings of the 4th International Conference Conference on Computer Systems and Technologies: E-Learning (CompSysTech '03)*, pp. 290–295, Jun. 2003.
- [18] Y. Bar-Shalom, F. Daum and J. Huang, "The probabilistic data association filter," *IEEE Control Syst. Mag.*, vol. 29, no. 6, pp. 82–100, Dec. 2009.
- [19] S. S. Blackman and R. Popoli, *Design and analysis of modern tracking systems*, Artech House, 1999.
- [20] R. Badeau, G. Richard, and B. David, "Adaptive ESPRIT algorithm based on the PAST subspace tracker," *IEEE Int. Conf. Acoustics Speech and Signal Processing (ICASSP)*, pp. 229–232, 2003.
- [21] J. Q. Lin, and S. C. Chan, "A new PAST-based adaptive ESPRIT algorithm with variable forgetting factor and regularization," *IEEE 23rd Int. Conf. Digital Signal Process. (DSP)*, pp. 1–5, 2018.
- [22] S. Li, J. Lv and S. Tian, "Posterior Cramer-Rao lower bound for wireless sensor localisation networks," *Electron. Lett.*, vol. 54, no. 22, pp. 1296–1298, 2018.